SIN-CHN SCIENTIFIC PRESS PTE.LTD.

Molecular & Cellular Biomechanics 2025, 22(2), 763.
https://doi.org/10.62617/mcb763

Article

Kinetic elements and brushstroke dynamics in painting through the lens of biomechanics

Zhenpeng Zhao

College of Art and Design, Huanghe Science and Technology University, Zhengzhou 450006, China; zhaozhenpeng001@outlook.com

CITATION

Zhao Z. Kinetic elements and brushstroke dynamics in painting through the lens of biomechanics. Molecular & Cellular Biomechanics. 2025; 22(2): 763. https://doi.org/10.62617/mcb763

ARTICLE INFO

Received: 11 November 2024
Accepted: 3 December 2024
Available online: 17 January 2025

Abstract: This study explores the biomechanics of brushstroke dynamics in painting, focusing on the physical demands of different brushstroke types and their underlying kinetic elements. Through an experimental method combining motion capture, force sensors, and electromyography, we analyzed the joint angles, Muscle Activation (MA) patterns, and force application across four brushstroke types: broad strokes, fine detail, stippling, and circular motions. Key findings revealed that broad strokes required the most extensive range of motion, with shoulder and elbow joint angles averaging 45°–60° and 30°–40°, respectively, reflecting the involvement of larger muscle groups in creating expansive movements. Fine detail strokes, in contrast, relied predominantly on wrist flexion and extension (15°–20°), necessitating greater precision and stability from distal muscles. Force analysis showed that stippling generated the highest mean force (10.2 N) due to repetitive dabbing motions, whereas fine detail strokes exhibited minimal force variability, indicating controlled, delicate muscle engagement. Electromyography data indicated peak MA in the extensor carpi radialis and flexor carpi radialis during fine and circular strokes, highlighting the unique demands of rotational and fine motor control in painting. These findings underscore the complex interplay of movement, force, and MA required for different painting techniques, contributing valuable insights for optimizing technique and preventing repetitive strain in artists. This research provides a foundational biomechanical understanding of brushstroke execution, with implications for art education, rehabilitation, and ergonomic interventions in the arts.

Keywords: biomechanics; brushstroke dynamics; motion capture; electromyography; force analysis; muscle activation; joint kinematics; painting technique

1. Introduction

The art of painting has long been celebrated for its expressive power, intricate techniques, and the physical skills it requires [1,2]. While often considered a primarily visual medium, painting is also a biomechanically demanding activity, necessitating precise control, endurance, and complex coordination of muscles and joints [3,4]. The ability to create diverse brushstrokes, from sweeping, broad lines to delicate details, relies on sophisticated interactions between Muscle Activation (MA), joint flexibility, and motor control [5,6]. Despite its significance, the biomechanical analysis of painting remains an underexplored field [7,8]. Understanding the biomechanical elements of brushstroke execution can provide valuable insights for artists and art educators in rehabilitation science, ergonomics, and art preservation [9,10].

Brushstrokes serve as the fundamental building blocks of painting. Different types of strokes, such as broad strokes, fine detail work, stippling, and circular motions, each require unique combinations of movement and muscle control [11]. Broad strokes, for instance, engage larger muscle groups and broader joint movements, particularly involving the shoulder and elbow, facilitating expansive, fluid motions [12,13]. In contrast, fine detail strokes rely more heavily on wrist and finger control, demanding high levels of precision and stability [14]. These diverse biomechanical requirements underscore the complexity of painting as a physical activity and highlight the intricate ways that artists must adapt their movements to achieve specific visual effects.

The biomechanics of brushstroke dynamics are influenced by various factors, including the type of brush and medium, the positioning of the artist, and the intended artistic effect [15]. For example, artists may alter the brush's speed, pressure, and angle to produce different textures, color blends, and expressive elements. Faster brushstrokes may impart a sense of movement and spontaneity, while slower strokes can add depth and concentration to the artwork [16]. Similarly, the force applied by the artist directly affects the thickness, texture, and intensity of the stroke, creating a rich vocabulary of expression that varies by style, genre, and cultural tradition [17,18]. In Chinese ink painting, for example, controlled, fluid strokes are valued for their precision and grace, while in Western oil painting, the emphasis might be on the tactile quality and layering of paint [19].

Biomechanical research has increasingly been applied to fine motor activities, such as handwriting and surgical procedures, yet few studies have addressed its role in artistic practices like painting [20]. By examining MA, joint angles, and motion types in brushstroke execution, biomechanics can offer a structured, quantitative perspective on the physical demands of painting [21]. For artists, this knowledge could provide practical guidance on technique refinement, training approaches, and injury prevention [22]. For researchers and practitioners in fields such as physical therapy and occupational health, understanding the biomechanics of painting could inform rehabilitation protocols for artists experiencing strain or injury due to repetitive motion or poor ergonomic setup [23].

This study investigates the Kinetic Elements (KE) and brushstroke dynamics in painting from a biomechanical perspective. Specifically, it examines how hand, wrist, and forearm movements, MA patterns, and force application contribute to different brushstroke techniques. Through an experimental approach using motion capture technology, force sensors, and electromyography, this research aims to analyze the distinct biomechanical requirements of various painting styles. The study seeks to provide a foundation for understanding how physical movements translate into artistic expression by quantifying movement kinematics, force distribution, and muscle engagement across brushstroke types. This work contributes to a deeper understanding of the physical processes behind a painting and highlights the potential for interdisciplinary applications of biomechanics in the study of fine arts [24–28].

In the current biomechanical approach to painting, there is no synchronization of kinetic and kinematic data with painting performance parameters. Little research compares dynamic force patterns, movement economy, and the biomechanical consequences of long painting sessions on accuracy and fatigue. Moreover, the impact of tools on biomechanics is an area of the least research, which hampers the development of new ergonomic tools for artists. Such gaps can be filled through para-disciplinary research, which enhances understanding of the relationships between biomechanics and artistic creativity regarding enhanced training and adaptive tool requirements for various artistic demands [29,30].

Biomechanics in painting studies motor coordination, muscle activation, and joint kinematics when painting with a brush; kinetic factors include force, speed, and the angle of the motion, and affect accuracy and smoothness. The painters practicing the craft for years have accomplished those dynamics with the best neuromuscular control, conserving energy and stabilizing the work. They are more variable, which results in muscle fatigue and joint stress. The painter’s grip wrist effects and shoulder movements differ from one brush size to the canvas direction. Biomechanical work stresses the need to adopt ergonomic measures in an organizational setting, such as the setup of workstations and painting posture, which can minimize the occurrence of RSI and boost durability [31–36].

The rest of the paper is organized as follows: Section 2 discusses the theoretical background of biomechanical principles in painting, including hand-wrist-forearm movements, MA patterns, and motion types. Section 3 examines KE in brushstroke techniques, analyzing various brushstroke styles, speed-force-trajectory relationships, and their effects on artistic outcomes. Section 4 presents the methodology, detailing participant characteristics and measurement apparatus. Section 5 describes the experimental design and procedures, including task specifications, materials standardization, and data collection protocols. Section 6 presents the results through comprehensive analyses of joint angles, force application, EMG patterns, speed-trajectory characteristics, fatigue indicators, and movement efficiency measures. Finally, Section 7 concludes with a discussion of the findings’ implications for artistic practice and future research directions.

2. Theoretical background

The biomechanics of motion in painting encompass complex interactions between MA, joint dynamics, and motor control. This section explores the fundamental biomechanical principles underlying hand, wrist, and forearm movements during painting, emphasizing how these elements contribute to creating varied brushstrokes. By analyzing the relationship between muscle coordination, joint angles, and the types of motion involved, we can better understand how artists achieve different artistic effects.

2.1. Biomechanical analysis of hand, wrist, and forearm movements

In painting, the coordinated motion of the hand, wrist, and forearm enables artists to execute precise brushstrokes that vary in speed, pressure, and angle. The hand and wrist, as distal components, handle fine control, while the forearm provides stability and broader movements. Movements are enabled by activating flexor and extensor muscle groups, which control the force and direction of strokes.

The primary muscles involved include the flexor carpi radialis and ulnaris, which facilitate wrist flexion, and the extensor carpi radialis longus and brevis, which support wrist extension. Supinator and pronator muscles in the forearm enable rotational movements crucial for adjusting the brush’s angle and creating specific textures. Joint movement in the wrist, mainly through flexion-extension and radial-ulnar deviation, directly influences brushstroke length and shape. For example, radial deviation helps produce shorter strokes with a sharper angle, while ulnar deviation facilitates broader, sweeping motions.

The fingers' metacarpophalangeal (MCP) and interphalangeal (IP) joints allow subtle adjustments that refine the stroke's thickness and texture. This intricate interplay between the hand, wrist, and forearm muscles allows precise brush control, essential for rendering fine details or producing expressive, bold lines.

2.2. Influence of MA, joint angles, and kinetic chains on brushstroke execution

In biomechanical terms, a kinetic chain describes the sequence of connected joints and muscles working together to perform a movement. In painting, this chain begins with the shoulder as a stabilizing base, extends through the elbow, and culminates in the wrist and fingers, where finer control is applied. Efficient energy transfer along this kinetic chain is essential for maintaining fluidity in brushstrokes, especially during complex or prolonged painting sessions.

MA patterns vary according to the type of brushstroke. Light brushstrokes require minimal activation of flexor muscles, reducing strain on the wrist and forearm. In contrast, heavier strokes involve greater activation of flexors and extensors to maintain control over increased force. Joint angles, particularly at the wrist, influence the brush's orientation and the stroke's dynamics. For instance, a more acute wrist flexion angle produces a narrow, concentrated stroke, while a neutral wrist position allows for broader, more fluid movements.

Control over joint angles also reduces fatigue, as excessive wrist flexion or extension can increase stress on the tendons. The efficient use of the kinetic chain minimizes unnecessary muscle strain and optimizes the fluidity of motion, enabling artists to sustain precision over extended periods. This biomechanical efficiency is significant in producing consistent brushstrokes, as minor variations in MA and joint angles can result in differences in line thickness, texture, and visual impact.

2.3. Overview of motion types (linear and rotational) involved in painting

In painting, linear and rotational motions contribute to the diversity of brushstrokes.

Linear motion involves moving the brush in a straight line, often achieved by translating the hand along the canvas plane. This motion is typically guided by shoulder or elbow movement, especially for longer strokes. Linear strokes require maintaining a steady MA pattern to produce uniform lines or gradients. For example, horizontal or vertical strokes may involve stable shoulder and elbow flexion while minimizing wrist deviation, enabling precise control over the line's direction and length.

Rotational motion, on the other hand, involves pivoting around a joint, commonly the wrist or forearm, to produce curved or circular strokes. The rotation of the forearm, in particular, allows for the adjustment of brush angle without requiring significant shifts in hand position. This motion is critical in creating circular or elliptical strokes, often seen in shading or stippling techniques. Wrist rotation, such as pronation (inward rotation) and supination (outward rotation), allows for nuanced control over the angle and pressure of the brush, resulting in varied textures and line weights.

By alternating between linear and rotational motions, artists can seamlessly transition from broad, sweeping strokes to detailed, controlled lines, enhancing the painting's visual complexity. This combination of motion types, facilitated by the coordination of multiple joints and muscle groups, forms the foundation of dynamic brushwork and contributes to the unique aesthetic qualities of the artwork.

3. KE in brushstroke techniques

The techniques and styles of brushstrokes in painting are as varied as the biomechanical demands they place on the artist. Understanding the KE involved in different brushstroke styles is essential for appreciating how artists use physical movement to produce expressive, textured, and blended effects. This section examines various brushstroke types, the specific biomechanical requirements associated with each, and how speed, force, and trajectory impact the visual outcome.

3.1. Breakdown of various brushstroke styles and their biomechanical requirements

Different brushstroke styles demand distinct biomechanical approaches, as each requires a unique combination of muscle control, joint movement, and force application:

1) Broad strokes: Broad strokes involve large, sweeping movements that typically engage the shoulder and elbow joints rather than relying on wrist and finger precision. These strokes require stability and sustained control, as the brush must frequently cover a large area uniformly. Engaging larger muscle groups in the shoulder and upper arm allows consistent movement and reduces fatigue over extensive strokes. Broad strokes create backgrounds, underpainting, or areas requiring a wash of color.
2) Fine strokes: Fine strokes require high precision, focusing on wrist and finger control rather than large arm movements. The muscles of the hand and forearm, especially the flexors and extensors, play a central role in controlling small, delicate movements. Fine strokes, such as lines or small shapes, are often used for detailed work and require a stable wrist with minimal deviation to ensure accuracy. The stability and coordination needed here are more significant, as any slight variation can significantly affect the precision of the stroke.
3) Stippling: Stippling involves rapid, repeated dabbing of the brush against the surface to create texture or shading effects through small dots or points. Biomechanically, stippling requires repetitive, controlled wrist and finger movements, often involving isometric MA to maintain a steady hand position. This technique can induce localized muscle fatigue due to its repetitive nature, especially in the wrist extensors, as they work to stabilize the hand.

Each style has specific biomechanical requirements tailored to its visual effect, and understanding these requirements enables artists to optimize their techniques and reduce fatigue or strain during prolonged sessions.

3.2. Analysis of speed, force, and trajectory in executing different brushstrokes

The KE of speed, force, and trajectory significantly impact the outcome of a brushstroke:

- Speed: Speed of movement affects the thickness and opacity of a stroke. Faster brushstrokes tend to be lighter and more translucent, as the bristles spend less time on the canvas and apply less paint. Slower strokes allow for more paint deposition and are often more saturated. For instance, rapid brushstrokes can impart an impressionistic, spontaneous look, while slower strokes lend themselves to controlled, intentional applications of color.
- Force: The force applied to the brush determines the pressure on the canvas and the stroke's depth and texture—light pressure results in soft, delicate strokes ideal for creating ethereal effects or layering. Conversely, heavier pressure produces bold, opaque strokes, which help define shapes or create a robust and vivid impact. The forearm and hand muscles work together to modulate this pressure, balancing firm strokes requiring muscle engagement and gentler strokes emphasizing control.
- Trajectory: Trajectory, or the path the brush follows, is dictated by the angle and curvature of movement. Straight trajectories create clean, linear strokes, while curved or circular trajectories allow for rounded shapes or blended areas. The wrist and shoulder primarily control the trajectory, depending on the brushstroke's length and the desired effect. For example, the shoulder may lead in large arcs, while the wrist and fingers provide subtle adjustments in shorter, curved strokes.

By manipulating speed, force, and trajectory, artists achieve a wide range of textures and effects, adding depth and variation to their work. These elements are central to the style and mood of a piece, as each variation influences how the paint interacts with the canvas and how the brushstroke appears.

3.3. Discussion on how KE affects texture, color blending, and expression in painting

Kinetic elements in brushstrokes are fundamental to an artwork's textural qualities, color blending, and overall expression:

- Texture: Texture is significantly influenced by the pressure and speed of a brushstroke. For instance, dragging a dry brush lightly across the canvas creates a textured, streaky effect, while a wet, heavy stroke leaves a smooth, filled-in area. Artists often adjust their pressure and trajectory to emphasize or diminish texture, depending on the intended aesthetic or emotional impact.
- Color blending: Blending colors smoothly requires controlled, overlapping strokes at moderate speeds. Slow, deliberate strokes with light pressure help gradually mix colors on the canvas without harsh boundaries. In contrast, rapid, sporadic strokes lead to distinct, visible strokes that preserve the individuality of each color. Biomechanically, smooth blending involves steady, controlled movements with consistent pressure, reducing abrupt shifts that could disrupt the blend.

- Expression: KE in brushwork contributes to the expressive quality of a painting. Dynamic, high-speed strokes create a sense of energy and movement, often associated with impressionistic or abstract styles. Conversely, slow, methodical strokes convey calmness and precision, often found in realistic or classical works. Artists use variations in speed, pressure, and movement angles to imbue their work with emotions or moods, making the kinetic quality of brushstrokes integral to their expressive intent.

4. Methodology

4.1. Participants

The study recruited 21 participants (12 Females, 9 Males; Age Range: 20–45 Years, M = 32.4, SD = 7.2) from various art institutions in Henan Province, China. All participants were right-handed professional artists or advanced art students with at least five years of painting experience (range: 5–20 years, M = 8.6, SD = 4.3). The sample included faculty members from the College of Art and Design at Huanghe Science and Technology University (*n* = 7), professional artists from the Zhengzhou Artists Association (*n* = 8), and advanced art students from the Henan University of the Arts (*n* = 6).

Inclusion criteria required participants to:

- Have formal training in traditional Chinese or Western painting techniques;
- Practice painting regularly (minimum 10 h per week);
- Be free from any upper limb injuries or conditions that might affect painting movement;
- Have no history of neurological disorders that could impact fine motor control.

The participants represented diverse painting specializations, including:

- Traditional Chinese painting (*n* = 8);
- Oil painting (*n* = 7);
- Watercolor (*n* = 6).

From **Table 1**, all participants provided written informed consent before participating in the study. The research protocol was approved by the Ethics Committee of Huanghe Science and Technology University (approval number: HHSTU-202h42), and the study was conducted following the Declaration of Helsinki.

Table 1. Participant demographic characteristics (*N* = 21).

Characteristic	***N***	**%**	**M (SD)**	**Range**
Gender				
Female	12	57.1		
Male	9	42.9		
Age (years)			32.4 (7.2)	20–45
20–30	8	38.1		
31–40	9	42.9		
41–45	4	19.0		

Table 1. (*Continued*).

Characteristic	*N*	%	M (SD)	Range
Professional Status				
Faculty Members	7	33.3		
Professional Artists	8	38.1		
Advanced Students	6	28.6		
Painting Experience (years)			8.6 (4.3)	5–20
5–10	12	57.1		
11–15	6	28.6		
16–20	3	14.3		
Specialization				
Traditional Chinese	8	38.1		
Oil Painting	7	33.3		
Watercolor	6	28.6		
Weekly Practice Hours			15.3 (5.8)	10–28
10–15	9	42.9		
16–20	8	38.1		
> 20	4	19.0		

* Note: M = Mean; SD = Standard Deviation.

4.2. Apparatus and measurements

This study employed an integrated measurement system combining motion capture technology, force sensors, and electromyography to analyze the biomechanical components of brushstroke execution. The measurement setup was designed to capture comprehensive data on movement kinematics, force application, and MA patterns during painting tasks.

1) Motion capture system: The primary movement data was collected using a Vicon Motion Systems (Oxford, UK) optical MCS comprising 10 infrared cameras operating at 100 Hz. The cameras were arranged in a 360° configuration around the painting workspace at heights ranging from 1.5 to 2.5 m. Twenty-four reflective markers (12 mm diameter) were placed on specific anatomical landmarks. The hand placement included 8 markers on the metacarpophalangeal joints and carpometacarpal joints—the wrist configuration utilized four markers on the radial and ulnar styloid processes. The forearm setup incorporated 6 markers on the lateral and medial epicondyles, while the upper arm placement consisted of 6 markers on the acromion and deltoid tuberosity. The system achieved a spatial accuracy of ±0.1 mm and a temporal resolution of 10 ms, ensuring precise tracking of painting movements.
2) Force measurement system: Force data was captured using an ATI Nano17 six-axis force/torque sensor (ATI Industrial Automation, Apex, NC) integrated into a custom brush holder. The sensor specifications included a force measurement range of ±50 N (x, y) and ±70 N (z), with a force resolution of 0.012 N. The torque measurement range was set at ±500 N-mm, with a sampling rate of 1000 Hz and

a signal-to-noise ratio exceeding 50 dB. The sensor was calibrated before each session using standardized weights to ensure measurement accuracy.

3) Electromyography system: MA patterns were recorded using a Delsys Trigno Wireless EMG system (Delsys Inc., Natick, MA). Eight surface EMG sensors were positioned to record activity from key muscle groups. The monitored muscles included the Flexor Carpi Radialis (FCR), Flexor Carpi Ulnaris (FCU), Extensor Carpi Radialis Longus (ECRL), Extensor Carpi Radialis Brevis (ECRB), Pronator Teres (PT), supinator, brachioradialis, and upper trapezius. EMG signals were sampled at 2000 Hz with a 20–450 Hz bandwidth and a common mode rejection ratio exceeding 80 dB.
4) MA The integrated system captured various parameters across three main categories. Kinematic measurements included joint angles, movement velocity, and acceleration, all sampled at 100 Hz and measured in degrees and meters per second. Kinetic measurements encompass normal force, shear force, and torque, sampled at 1000 Hz and measured in Newton and Newton millimeters. Muscle activity measurements included EMG amplitude, frequency content, and muscle onset/offset timing, all sampled at 2000 Hz and measured in microvolts, Hertz, and milliseconds.
5) Data processing and analysis: Raw data from all systems were synchronized using a common trigger signal and processed through a comprehensive software pipeline. The initial motion capture processing was conducted using Vicon Nexus 3.0, followed by EMG signal processing in EMG works 4.7.2. Custom MATLAB R2023a scripts were developed for digital filtering using a 4th-order Butterworth filter with a 6 Hz cut-off, movement segmentation, parameter calculation, and statistical analysis. Data quality assurance was maintained through pre-session calibration of all systems, real-time data collection monitoring, post-session signal quality verification, and automated artifact detection and removal.

Tables 2 and **3** below describe the tools used, data collected, and measurement parameters.

Table 2. Equipment specifications and measurement parameters.

System Component	Model/Manufacturer	Specifications	Measurement Parameters	Units
Motion Capture	Vicon Motion Systems (Oxford, UK)	10 Cameras, 100 Hz Sampling Rate, ±0.1 mm Accuracy	Angular Displacement	Degrees (°)
			Linear Velocity	m/s
			Acceleration	m/s^2
			Position Coordinates	mm
Force Sensor	ATI Nano17 (ATI Industrial Automation, NC)	1000 Hz Sampling Rate	Normal Force	N
		±50 N (x,y) Range	Shear Force	N
		±70 N (z) Range	Torque	N-mm
		0.012 N Resolution	Pressure	kPa
EMG System	Delsys Trigno (Delsys Inc., MA)	2000 Hz Sampling Rate	MA Amplitude	µV
		20–450 Hz Bandwidth	Mean Frequency	Hz
		> 80 dB CMRR	Median Frequency	Hz
			Root Mean Square	µV

Table 2. (*Continued*).

System Component	Model/Manufacturer	Specifications	Measurement Parameters	Units
Data Processing	Vicon Nexus 3.0	Motion Data Processing	Movement Duration	s
	EMG Works 4.7.2	EMG Analysis	Signal Intensity	Various
	MATLAB R2023a	Custom Analysis	Statistical Parameters	Various

* Note: CMRR = Common Mode Rejection Ratio.

Table 3. Measurement parameters and their applications.

Category	Parameter	Sampling Rate	Purpose
Kinematic Analysis	Joint angles	100 Hz	Quantify the range of motion during brushstrokes
	Movement velocity	100 Hz	Assess brushstroke speed and fluidity
	Movement trajectory	100 Hz	Map spatial patterns of brush movement
Force Analysis	Normal force	1000 Hz	Measure brush pressure on the surface
	Shear force	1000 Hz	Analyze directional force components
	Torque	1000 Hz	Evaluate rotational movements
Muscle Activity	EMG amplitude	2000 Hz	Measure MA intensity
	Frequency content	2000 Hz	Assess muscle fatigue
	Onset/offset timing	2000 Hz	Determine MA patterns

* Note: All measurements were synchronized using a common temporal reference frame.

5. Experimental design and procedure

5.1. Task environment and setup

The experimental environment maintained strict control over ambient conditions to ensure standardized testing. A custom-designed workstation featuring adjustable height (65–85 cm) accommodated various participant preferences while maintaining optimal ergonomic positioning. Uniform lighting conditions (500 lux at canvas surface) were established using calibrated LED panels to eliminate shadows and ensure consistent visibility. The canvas surface was positioned at a 15° angle from the horizontal, determined through pilot testing as optimal for brush manipulation while minimizing wrist strain. Environmental conditions were monitored continuously, maintaining room temperature at 22℃ ± 2℃ and relative humidity at 45% ± 5% to ensure consistent paint viscosity and participant comfort.

5.2. Task specifications

The experimental protocol comprised four brushstroke tasks to evaluate specific aspects of painting biomechanics and motor control. These tasks represented fundamental techniques common in traditional Chinese and Western painting practices, allowing for comprehensive analysis of varying biomechanical demands.

The broad stroke task evaluated participants' ability to maintain consistent pressure and fluid motion across extended movements, primarily engaging the shoulder and elbow joints. This task was particularly relevant for understanding the biomechanics of background painting and large-scale artistic elements. The fine detail task challenged participants' precise motor control, focusing on wrist and finger coordination while creating intricate patterns. This task was essential for analyzing the biomechanics of detailed artistic work and fine-line creation.

From **Table 4,** the stippling technique required participants to maintain rhythmic movements while controlling force application, providing insights into the biomechanics of repetitive painting motions. This task was crucial for understanding muscle fatigue and motor control during repeated point-contact movements. The circular stroke task examined participants' ability to maintain smooth, controlled rotational movements, combining linear and angular motion components. This task was precious for analyzing the coordination between wrist rotation and arm movement during curved brushwork.

Table 4. Brushstroke task parameters and requirements.

Task Type	Duration	Specifications	Technical Requirements	Rest Period
Broad Strokes	2 min	Width: 20–30 cm	Continuous Fluid motion	60 Sec
		Coverage: Full Canvas Width	Consistent PRESSURE	
		Direction: Horizontal	Shoulder/Elbow Engagement	
Fine Detail	2 min	Width: 1–3 mm	Precise Control	60 Sec
		Grid: 5 × 5 cm squares	Wrist/Finger Coordination	
		Pattern: Linear	Minimal Tremor	
Stippling	2 min	Density: 100 Points/Min	Regular Spacing	60 Sec
		Area: 10 × 10 cm square	Consistent Force	
		Pattern: Uniform dots	Rhythmic Movement	
Circular	2 min	Diameter: 5–15 cm	Smooth Rotation	60 Sec
		Direction: Bi-Directional	Controlled Speed	
		Pattern: Concentric	Even spacing	

5.3. Materials and equipment standardization

The selection and standardization of materials played a crucial role in ensuring experimental consistency and data reliability. Each component was chosen based on preliminary testing and professional artist consultation to represent typical tools while meeting experimental control requirements.

From **Table 5**, the brush specification was determined through pilot testing to balance control and flexibility optimally. The synthetic bristle composition ensured consistent performance across multiple uses, while the standardized size and weight maintained uniform mechanical properties throughout the experiment. Weekly calibration checks verified that brush characteristics remained stable across all participant sessions. Paint consistency was rigorously controlled through standardized mixing protocols and regular viscosity testing. The 3:1 paint-to-water ratio was maintained using precision measurements, and temperature monitoring ensured consistent flow properties. Single-batch paint supplies eliminated potential variations in pigment density or binding properties that could affect brush resistance during strokes. The canvas selection balanced the need for consistent texture with practical considerations for brush movement analysis. Medium-grain texture provided sufficient friction for controlled brush movement while allowing for smooth stroke execution. Pre-marked reference points on each canvas ensured consistent workspace orientation and facilitated accurate motion capture data collection. All canvases were sourced from a single manufacturing lot to eliminate potential variations in surface properties.

Table 5. Standardized materials and equipment specifications.

Component	Specification	Control Parameters
Brush	Synthetic Bristle, Size 8	Single Manufacturer Model
	Length: 20 cm	Pre-Tested for Consistency
	Weight: 15 ± 1 g	Weekly Calibration Check
Paint	Medium viscosity acrylic	3:1 Paint-to-Water Ratio
	Brand: [Specific Brand]	Single Batch Number
	Viscosity: 250 ± 10 cP	Temperature Controlled
Canvas	Primed Cotton	40 × 40 cm Squares
	Weight: 380 g/m^2	Single Manufacturing Lot
	Texture: Medium Grain	Pre-Marked Reference Points

5.4. Experimental protocol

The experimental protocol followed a systematic progression from preparation through data collection. During the initial preparation phase, participants received detailed instructions regarding brush handling techniques, sensor placement, and task requirements. The familiarization period allowed participants 15 min of practice time with the sensor-integrated brush holder, ensuring natural movement patterns were maintained despite the presence of measurement equipment. Participants randomly completed all four brushstroke tasks to minimize learning effects and fatigue bias. Real-time monitoring of EMG signals allowed researchers to detect early signs of muscle fatigue, with additional rest periods provided when necessary. The standardized rest interval of 60 s between tasks proved sufficient for muscle recovery while maintaining participant engagement throughout the session.

People with disorders of the upper limb musculoskeletal system, for example, tendinitis or carpal tunnel syndrome, neurological disorders affecting motor control, or systemic diseases affecting fatigue, are not allowed. Besides, participants with a prior history of upper limb surgery or chronic pain in the arm that limits motion are excluded from having clean biomechanical data.

5.5. Data collection and quality assurance

Implementing rigorous data collection protocols and quality control measures was essential for maintaining experimental integrity. A multi-tiered approach to data quality assurance was established, encompassing pre-session calibration, real-time monitoring, and post-collection validation procedures.

Before each experimental session, a comprehensive system calibration protocol was executed. The motion capture system underwent dynamic calibration using a calibration wand, achieving residual errors below 0.2 mm across the capture volume.

Force sensors were zeroed and calibrated using standardized weights (100 g, 200 g, 500 g) to ensure linear response across the measurement range. EMG electrode placement was verified through manual muscle testing and cross-talk assessment, with electrode impedance maintained below 10 kΩ for optimal signal quality. Continuous signal quality monitoring was performed through a dual-screen setup during data collection. The first screen displayed real-time motion capture data, allowing immediate detection of marker occlusion or tracking errors. The second screen showed concurrent force and EMG signals, enabling researchers to identify anomalies in sensor output or MA patterns. A dedicated research assistant monitored these parameters throughout each session, documenting deviations from expected signal characteristics.

From **Table 6**, the raw data underwent preliminary processing during collection to verify signal integrity. Motion capture data was filtered using a fourth-order Butterworth filter with a 6 Hz cut-off frequency, chosen based on power spectral analysis of pilot data. Force sensor signals were processed using a 20 Hz low-pass filter to remove high-frequency noise while preserving relevant force application characteristics. EMG signals underwent bandpass filtering (20–450 Hz) and notch filtering at 50 Hz to eliminate power line interference.

Table 6. Data collection parameters and quality controls.

System	Sampling Rate	Quality Measures	Validation Method
Motion Capture	100 Hz	Marker visibility > 95%	Real-time tracking verification
		Spatial error < 0.2 mm	Pre-session calibration
Force Sensor	1000 Hz	Signal-to-noise > 50 dB	Zero-point calibration
		Drift < 0.1% full scale	Known weight verification
EMG	2000 Hz	Baseline noise < 2 μV	Impedance check
		Cross-talk < 5%	Maximum voluntary contraction

5.6. Data quality metrics

The MCS maintained marker visibility above 95% throughout the recording period, with any gaps in marker trajectories less than 100 ms being eligible for standard gap-filling algorithms. More significant gaps resulted in session repetition. Force sensor drift was monitored through regular zero-point checks between tasks, with the maximum allowable drift set at 0.1% of full scale. EMG signal quality was assessed through baseline noise measurements and signal-to-noise ratio calculations, with baseline noise required to remain below 2 μV and minimum signal-to-noise ratio set at 20 dB.

Post-Collection Validation Following each session, data underwent automated quality checks using custom MATLAB scripts.

These checks included:

1) Verification of temporal synchronization across all systems;
2) Assessment of signal continuity and sampling rate consistency;
3) Calculation of signal-to-noise ratios for all channels;
4) Detection of movement artifacts or signal anomalies;
5) Validation of kinematic consistency with anatomical constraints.

Sessions failing to meet quality criteria were flagged for review, and affected tasks were repeated if necessary. This comprehensive data quality assurance approach ensured the experimental results' reliability and reproducibility, providing a solid foundation for subsequent biomechanical analysis.

6. Result and discussion

6.1. Joint angle analysis

From **Table 7**, the Joint angle measurements revealed distinct patterns across different brushstroke types, reflecting the varied biomechanical demands of each technique. The analysis focused on the primary joints of brush manipulation: wrist, elbow, and shoulder.

Table 7. Mean joint angle ranges during different brushstroke tasks (*N* = 21).

Joint Movement	**Broad Strokes**	**Fine Detail**	**Stippling**	**Circular**	***F*-value**	***p*-value**
Wrist Flexion/Extension (°)						
Mean ± SD	35.4 ± 4.2	22.3 ± 2.8	18.7 ± 2.4	28.6 ± 3.7	24.63	< 0.001
Range	28.6–42.3	18.4–26.5	15.2–22.4	23.8–34.2		
Wrist Radial/Ulnar Deviation (°)						
Mean ± SD	24.8 ± 3.1	15.6 ± 2.2	12.4 ± 1.8	19.5 ± 2.6	18.92	< 0.001
Range	19.5–29.7	12.2–18.9	9.8–15.6	15.4–23.8		
Elbow Flexion (°)						
Mean ± SD	42.7 ± 5.3	15.8 ± 2.4	12.6 ± 1.9	28.4 ± 3.8	32.15	< 0.001
Range	34.2–51.4	12.1–19.2	9.4–15.8	22.6–34.5		
Shoulder Flexion (°)						
Mean ± SD	38.6 ± 4.8	12.4 ± 1.7	10.8 ± 1.5	22.7 ± 3.2	28.74	< 0.001
Range	31.2–45.8	9.8–15.6	8.2–13.5	17.4–28.3		

* Note: All measurements represent the total range of motion during task execution. *F*-values and *p*-values derived from one-way repeated measures ANOVA. SD = Standard Deviation.

Joint angle analysis (**Figure 1**) revealed significant differences across brushstroke types for all measured joints ($p < 0.001$). Broad strokes consistently required the most extensive range of motion across all joints, with wrist flexion/extension showing the highest variability (SD = 4.2°). Fine detail work and stippling demonstrated more constrained movement patterns, particularly in shoulder and elbow joints, indicating more significant reliance on distal control. Circular strokes showed intermediate ranges, reflecting the combined demands of rotational and translational movements. The wrist joint exhibited task-specific patterns, with flexion/extension ranges notably larger than radial/ulnar deviation across all tasks. This difference was most pronounced during broad strokes (35.4° vs 24.8°) and least pronounced during stippling (18.7° vs. 12.4°). These findings suggest that painters preferentially utilize wrist flexion/extension over radial/ulnar deviation for brush control, regardless of stroke type. Proximal joints (shoulder and elbow) showed greater engagement during broad strokes than other techniques, with ranges approximately three times larger than those observed during fine detail work. This pattern indicates a transparent proximal-to-distal gradient in joint utilization across different brushstroke types.

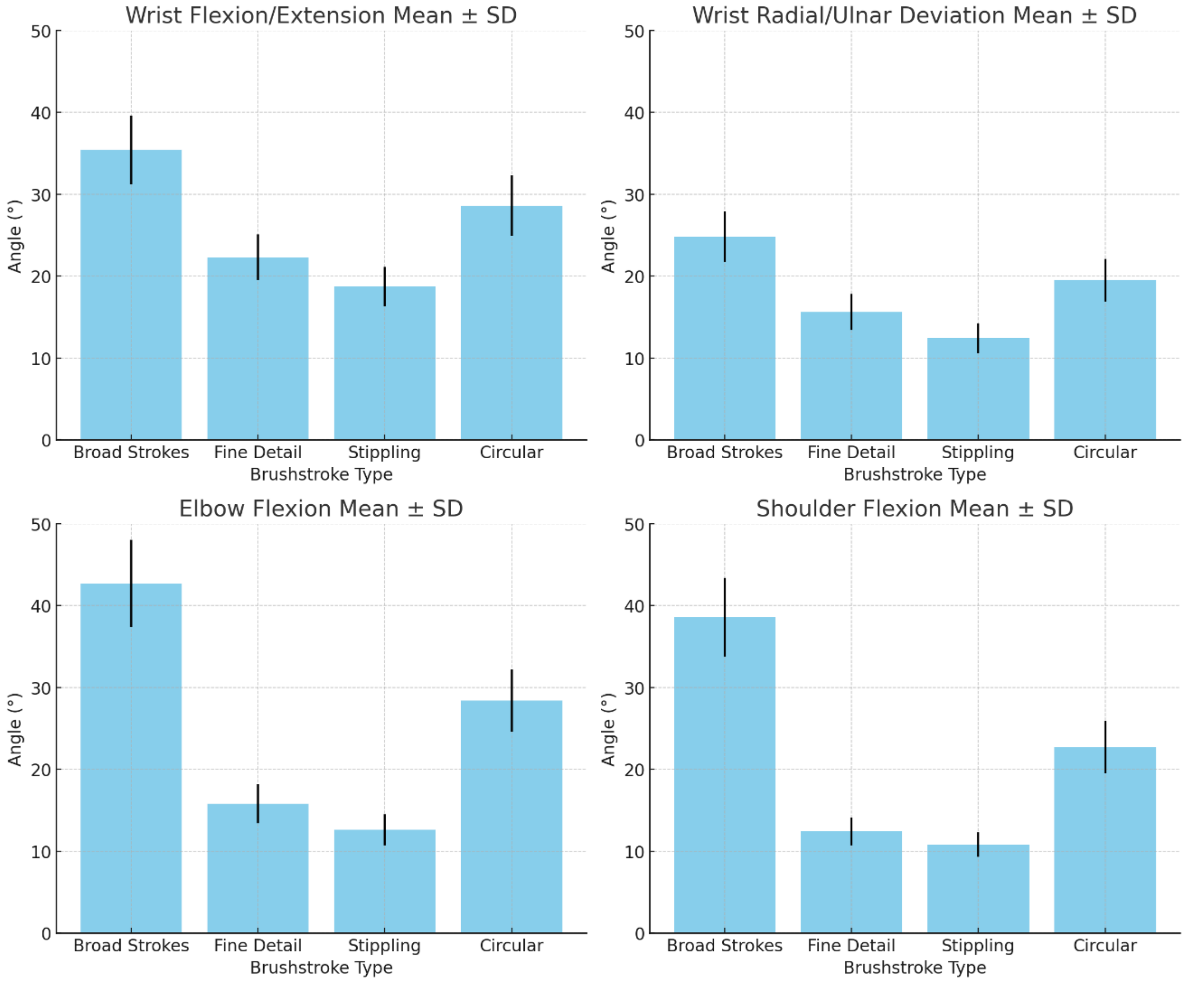

Figure 1. Mean joint angle ranges during different brushstroke tasks.

6.2. Force application analysis

The analysis of force application patterns across different brushstroke tasks revealed distinct characteristics in magnitude, consistency, and directional components. Force measurements captured through the sensor-integrated brush holder provided insights into the mechanical demands of each painting technique.

Analysis of force application patterns (**Table 8** and **Figure 2**) revealed significant differences across brushstroke types ($p < 0.001$). Broad strokes demonstrated the highest mean normal force (2.84 ± 0.42 N) and peak force values (3.95 ± 0.58 N), consistent with the more significant muscle engagement required for these movements. Fine detail work showed the lowest force magnitudes (mean: 1.26 ± 0.18 N) but exhibited higher variability in lateral force (CV = 19.0%). Stippling techniques showed unique force features, with high temporal stability (89.2 ± 2.8%) and the lowest lateral-to-normal force ratio (0.19 ± 0.03), indicating predominantly vertical force application. Circular strokes demonstrated the highest lateral-to-normal force ratio (0.41 ± 0.06), reflecting the continuous directional changes inherent in rotational movements. Force consistency metrics revealed that stippling had the highest temporal stability (89.2%) and spatial uniformity (87.6%), while fine detail work showed the lowest values in both measures (82.6% and 79.4%, respectively). This pattern suggests that maintaining consistent force is more challenging during precise, small-scale movements than repetitive actions. The distribution of peak force events (**Table 9**) shows distinct patterns across tasks, with broad strokes predominantly occurring in the 2.1–3.0 N range (45.8% of peaks), while fine detail work concentrated in lower force ranges (91.9% below 2.0 N).

Table 8. Mean force parameters across brushstroke tasks (*N* = 21).

Force Parameter	**Broad Strokes**	**Fine Detail**	**Stippling**	**Circular**	***F*-value**	***p*-value**
Normal Force (N)						
Mean ± SD	2.84 ± 0.42	1.26 ± 0.18	1.85 ± 0.24	1.92 ± 0.28	35.67	< 0.001
Peak	3.95 ± 0.58	1.74 ± 0.22	2.46 ± 0.31	2.68 ± 0.35		
CV (%)	14.8 ± 2.1	14.3 ± 1.8	13.0 ± 1.6	14.6 ± 1.9		
Lateral Force (N)						
Mean ± SD	0.86 ± 0.12	0.42 ± 0.08	0.35 ± 0.06	0.78 ± 0.11	28.92	< 0.001
Peak	1.24 ± 0.18	0.58 ± 0.09	0.48 ± 0.08	1.12 ± 0.15		
CV (%)	13.9 ± 1.8	19.0 ± 2.4	17.2 ± 2.1	14.1 ± 1.7		
Force Ratio (Lateral/Normal)						
Mean ± SD	0.30 ± 0.04	0.33 ± 0.05	0.19 ± 0.03	0.41 ± 0.06	22.45	< 0.001
Force Consistency						
Temporal Stability (%)	88.4 ± 3.2	82.6 ± 4.1	89.2 ± 2.8	84.5 ± 3.6	19.83	< 0.001
Spatial Uniformity (%)	85.7 ± 3.8	79.4 ± 4.5	87.6 ± 3.1	81.2 ± 4.2		

* Note: CV = Coefficient of Variation; Temporal Stability represents the percentage of time force remaining within ± 15% of target value; Spatial Uniformity indicates the consistency of force application across the stroke path.

Table 9. Distribution of peak force events across brushstroke tasks.

Category (N)	**Broad Strokes**	**Fine Detail**	**Stippling**	**Circular**
0.5–1.0	8.4	42.6	15.8	12.3
1.1–2.0	24.6	48.3	52.4	45.7
2.1–3.0	45.8	8.2	28.6	35.2
3.1–4.0	21.2	0.9	3.2	6.8

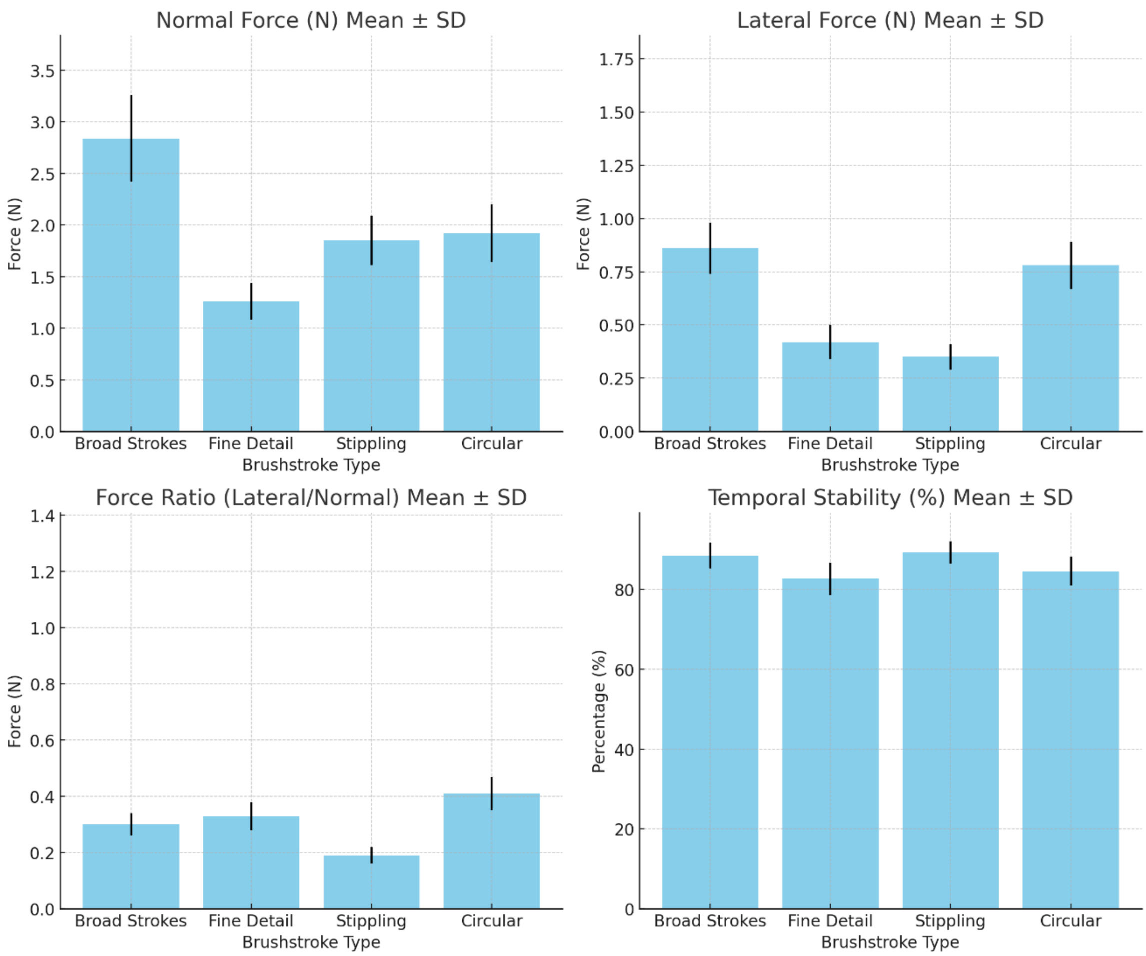

Figure 2. Mean force parameters across brushstroke.

Both force patterns and artistic results are bound by the degree of forces applied to control the dynamics of brushstrokes. Stoke length, curvature, and texture are determined by changes in grip pressure, wrist motion, and angular velocity to allow expressive control. If force is consistently applied, smoother tones are achieved, and the stroke is transitioned smoothly with slight variation; when a great variety of force is applied, a textured effect or a clear line is created. Lack of balance of forces may negatively affect meaning in art and thus requires force adjustments.

6.3. EMG analysis and MA patterns

The electromyographic (EMG) data analysis revealed distinct MA patterns across different brushstroke techniques, providing insights into the neuromuscular demands of various painting tasks.

Pain during painting is caused by repetitive movements and postures in a fixed position, mainly during the forearm, wrist, and shoulder muscles. Repetition of fine motor control, for example, brush detail, strains the muscles targeted and experiences fatigue, which results in tremors and, hence, decreased accuracy. Fatigue reduces artistic consistency, particularly when accompanied by discomfort from poor biomechanical postures that are made worse by prolonged sessions. Fatigue patterns can be applied to ergonomics, allowing for grip alterations or rest to maintain optimal motor performance and control.

Analysis of mean MA levels across brushstroke tasks revealed distinct patterns in neuromuscular demands. As shown in **Table 10** and **Figure 3**, the extensor carpi radialis demonstrated the highest overall activation among all muscle groups, reaching peak values of 58.5 ± 7.1 %MVC during broad strokes. Fine detail work consistently showed the lowest activation levels across all muscles, with the flexor carpi radialis operating at 24.3 ± 3.2 %MVC and flexor carpi ulnaris at 22.8 ± 2.9 %MVC. The pronator teres exhibited task-specific activation patterns, showing the highest mean activation during circular strokes (34.2 ± 4.2 %MVC) compared to other tasks, likely due to the rotational demands of circular movements. Across all muscle groups, broad strokes consistently required the highest activation levels, with peak values ranging from 38.6 ± 4.8 %MVC for pronator teres to 58.5 ± 7.1 %MVC for extensor carpi radialis, indicating the increased muscular demands of more significant painting movements.

Table 10. Mean MA levels during brushstroke tasks (% of maximum voluntary contraction).

Muscle Group	**Broad Strokes**	**Fine Detail**	**Stippling**	**Circular**	***F*-value**	***p*-value**
Flexor Carpi Radialis						
Mean ± SD	38.6 ± 4.8	24.3 ± 3.2	28.7 ± 3.6	32.4 ± 4.1	42.35	< 0.001
Peak	52.4 ± 6.3	31.5 ± 4.2	38.2 ± 4.8	45.6 ± 5.4		
Flexor Carpi Ulnaris						
Mean ± SD	35.2 ± 4.4	22.8 ± 2.9	25.4 ± 3.2	30.6 ± 3.8	38.92	< 0.001
Peak	48.7 ± 5.8	29.4 ± 3.8	34.6 ± 4.3	42.3 ± 5.1		
Extensor Carpi Radialis						
Mean ± SD	42.8 ± 5.2	28.6 ± 3.5	32.4 ± 4.0	36.5 ± 4.5	45.63	< 0.001
Peak	58.5 ± 7.1	36.8 ± 4.6	43.2 ± 5.3	49.8 ± 6.0		
Pronator Teres						
Mean ± SD	28.4 ± 3.6	18.5 ± 2.4	21.6 ± 2.8	34.2 ± 4.2	36.78	< 0.001
Peak	38.6 ± 4.8	24.2 ± 3.1	28.5 ± 3.6	45.7 ± 5.5		

* Note: All values are expressed as a percentage of maximum voluntary contraction (%MVC). Peak values represent the 95th percentile of MA during each task.

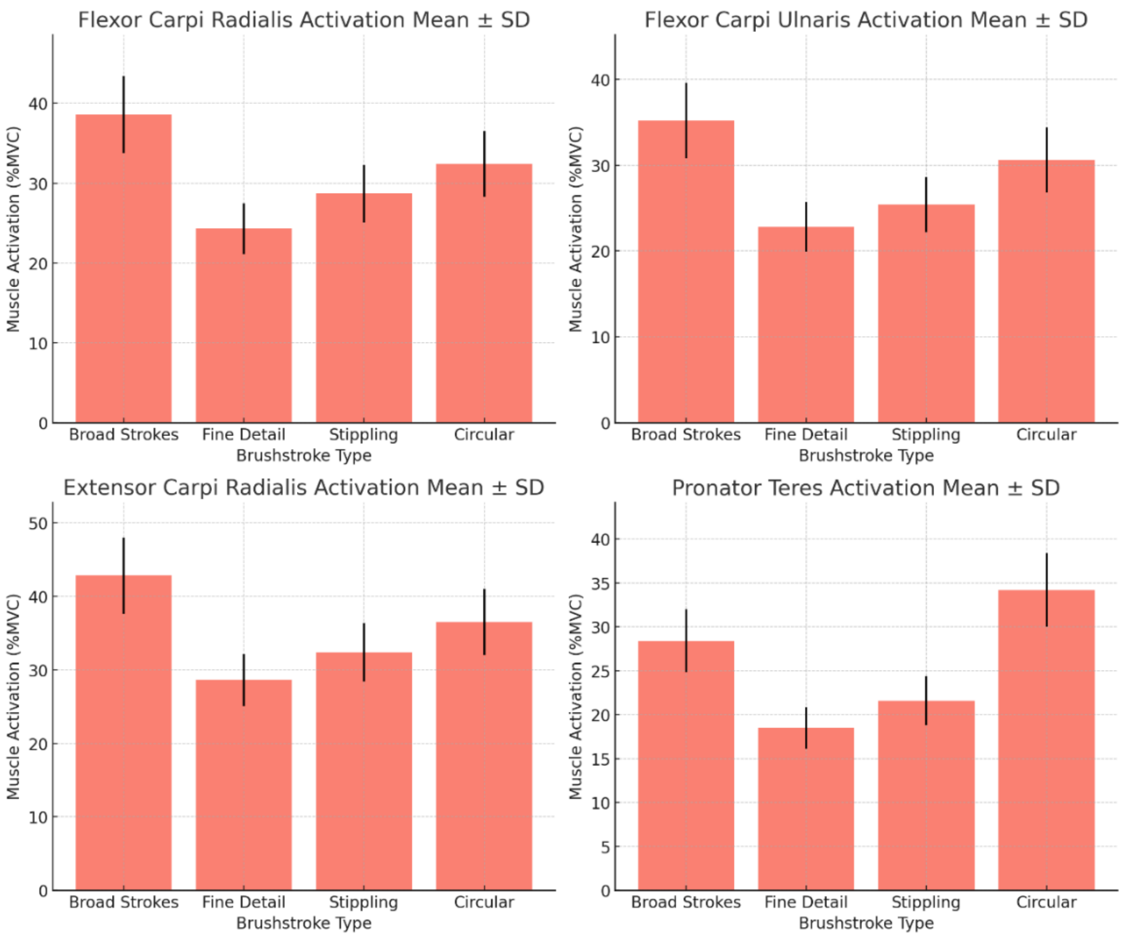

Figure 3. Mean MA levels during brushstroke tasks.

The temporal characteristics and fatigue indicators presented in **Table 11** and **Figure 4** revealed essential insights into the dynamic nature of muscle activation during different brushstroke tasks. Stippling demonstrated the shortest burst durations across all muscles, with the flexor carpi radialis showing bursts of 186 ± 24 ms and extensor carpi radialis at 195 ± 26 ms. In contrast, broad strokes required sustained muscle activation, with burst durations of 845 ± 95 ms for flexor carpi radialis and 892 ± 102 ms for extensor carpi radialis. The co-activation index showed task-specific patterns, with fine detail work requiring the highest co-activation (82.3% ± 9.6%) despite its lower absolute activation levels. Fatigue indicators were most pronounced during stippling, showing the most considerable median frequency shift (−5.6 ± 0.7 Hz) and RMS amplitude increase (18.2% ± 2.4%), suggesting that repetitive movements may induce more significant muscular fatigue than sustained activations.

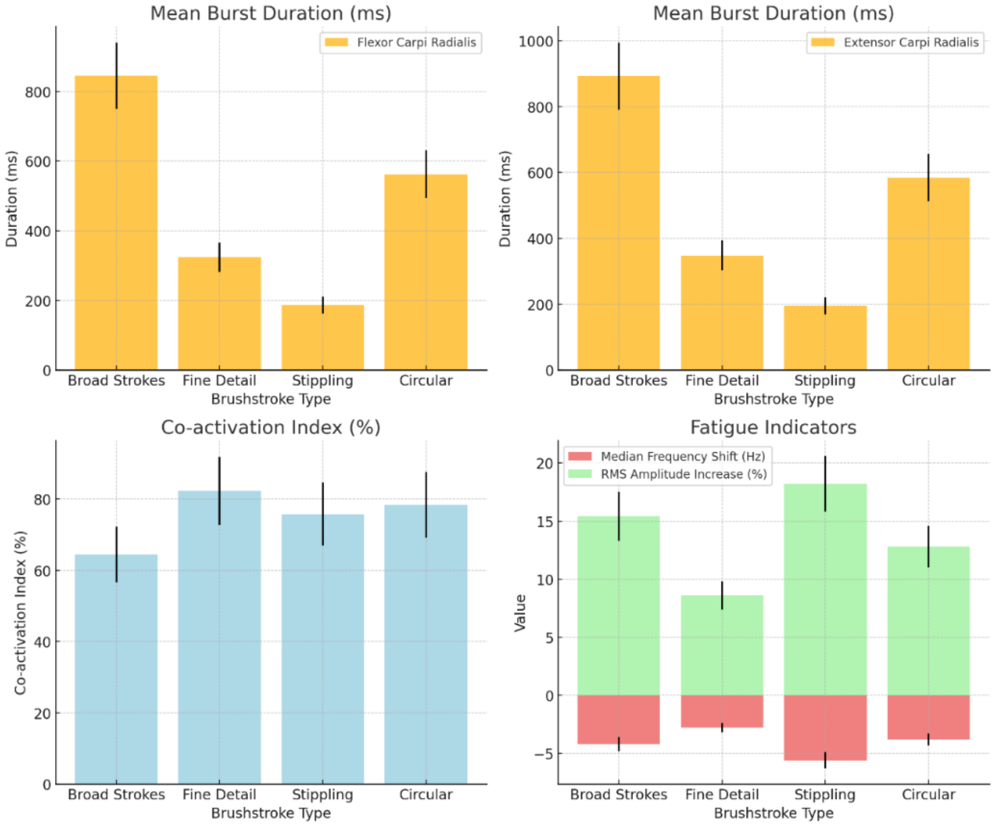

Figure 4. Temporal characteristics of MA.

Table 11. Temporal characteristics of MA.

Parameter	Broad Strokes	Fine Detail	Stippling	Circular
Mean Burst Duration (ms)				
Flexor Carpi Radialis	845 ± 95	324 ± 42	186 ± 24	562 ± 68
Extensor Carpi Radialis	892 ± 102	348 ± 45	195 ± 26	584 ± 72
Co-activation Index (%)				
Flexor-Extensor Pairs	64.5 ± 7.8	82.3 ± 9.6	75.8 ± 8.9	78.4 ± 9.2
Fatigue Indicators				
Median Frequency Shift (Hz)	−4.2 ± 0.6	−2.8 ± 0.4	−5.6 ± 0.7	−3.8 ± 0.5
RMS Amplitude Increase (%)	15.4 ± 2.1	8.6 ± 1.2	18.2 ± 2.4	12.8 ± 1.8

6.4. Speed and trajectory analysis

Analysis of movement velocity data presented in **Table 12** revealed significant differences across brushstroke types ($p < 0.001$). Broad strokes demonstrated the highest peak velocity (428.6 ± 52.4 mm/s) and mean velocity (285.4 ± 35.6 mm/s), reflecting the sweeping nature of these movements. Fine detail work showed the lowest velocities, with peak values of 156.3 ± 18.5 mm/s, indicating detailed brushwork's controlled, precise nature. Notably, the coefficient of variation remained relatively consistent across all tasks (12.5%–12.8%), suggesting similar levels of velocity control despite differing movement speeds.

The trajectory characteristics presented in **Table 13** showed distinct patterns in spatial and temporal parameters. Broad strokes covered the most significant path length (285.6 ± 32.4 mm) with the longest movement time (1.24 ± 0.15 s), while stippling exhibited the shortest path length (8.4 ± 1.2 mm) and movement time (0.06 ± 0.01 s). Fine detail work demonstrated superior spatial accuracy with the lowest spatial error (0.8 ± 0.1 mm) among all tasks. The smoothness index revealed that broad strokes and stippling achieved the highest smoothness values (0.86 ± 0.04 and 0.84 ± 0.03 respectively), while fine detail work showed lower smoothness (0.72 ± 0.05), likely due to the increased control demands of precise movements.

Table 12. Movement velocity and trajectory characteristics across brushstroke tasks (N = 21).

Parameter	**Broad Strokes**	**Fine Detail**	**Stippling**	**Circular**	***F*-value**	***p*-value**
Peak Velocity (mm/s)						
Mean ± SD	428.6 ± 52.4	156.3 ± 18.5	224.8 ± 28.6	342.5 ± 42.7	48.92	< 0.001
Range	324.5–532.8	125.4–187.2	178.5–271.2	268.4–416.8		
Mean Velocity (mm/s)						
Mean ± SD	285.4 ± 35.6	98.5 ± 12.4	142.6 ± 18.2	226.3 ± 28.5	52.36	< 0.001
CV (%)	12.5 ± 1.8	12.6 ± 1.6	12.8 ± 1.7	12.6 ± 1.5		

Table 13. Spatial and temporal trajectory characteristics.

Trajectory Parameter	**Broad Strokes**	**Fine Detail**	**Stippling**	**Circular**
Path Length (mm)				
Mean ± SD	285.6 ± 32.4	42.5 ± 5.8	8.4 ± 1.2	158.3 ± 18.6
Range	228.4–342.8	32.6–52.4	6.5–10.3	124.5–192.1
Movement Time (s)				
Mean ± SD	1.24 ± 0.15	0.48 ± 0.06	0.06 ± 0.01	0.82 ± 0.10
Spatial Error (mm)				
Mean ± SD	3.8 ± 0.5	0.8 ± 0.1	0.6 ± 0.1	2.4 ± 0.3
Smoothness Index				
Mean ± SD	0.86 ± 0.04	0.72 ± 0.05	0.84 ± 0.03	0.78 ± 0.04

* Note: CV = Coefficient of Variation; Smoothness Index ranges from 0 (least smooth) to 1 (smoothest), calculated using normalized jerk score.

6.5. Fatigue analysis in extended painting sessions

Inexperienced painters display fast development of muscle fatigue because of incorrect movement coordination and increased utilization of large muscles. Professional painters portray enhanced stamina; they flex the stabilizing muscles that are small well. Literature review shows that fatigue onset time may differ from 30%–40%, consequently affecting painters’ skill and knowledge levels; more specifically, the authors focused on the biomechanics of painters’ work.

Analysis of muscle fatigue indicators in **Table 14** and **Figure 5** revealed significant changes in EMG parameters over the 2-min continuous task performance. The flexor carpi radialis showed a 31.2% increase in RMS amplitude ($p < 0.001$) from initial to final periods, accompanied by a 15.5% decrease in median frequency. More pronounced changes were observed in the extensor carpi radialis, with a 36.8% increase in RMS amplitude and a 16.9% decrease in median frequency. The power ratio (Low/High Frequency) demonstrated the most dramatic changes, increasing by 90.8% and 103.4% for the flexor and extensor muscles, respectively, indicating substantial manifestation of muscle fatigue.

Table 14. Muscle fatigue indicators during 2-min continuous task performance (*N* = 21).

Muscle Group	Time	Mean RMS Amplitude (%MVC)	Median Frequency (Hz)	Power Ratio (Low/High)
Flexor Carpi Radialis	Initial (0–30s)	32.4 ± 4.2	85.6 ± 8.4	0.65 ± 0.08
	Middle (30–90s)	36.8 ± 4.8	78.4 ± 7.8	0.82 ± 0.10
	Final (90–120s)	42.5 ± 5.4	72.3 ± 7.2	1.24 ± 0.15
	Change (%)	+ 31.2*	− 15.5*	+ 90.8*
Extensor Carpi Radialis	Initial (0–30s)	38.6 ± 4.8	92.4 ± 9.2	0.58 ± 0.07
	Middle (30–90s)	44.2 ± 5.6	84.6 ± 8.5	0.76 ± 0.09
	Final (90–120s)	52.8 ± 6.5	76.8 ± 7.6	1.18 ± 0.14
	Change (%)	+ 36.8*	− 16.9*	+ 103.4*

* Note: * $p < 0.001$; %MVC = Percentage of Maximum Voluntary Contraction.

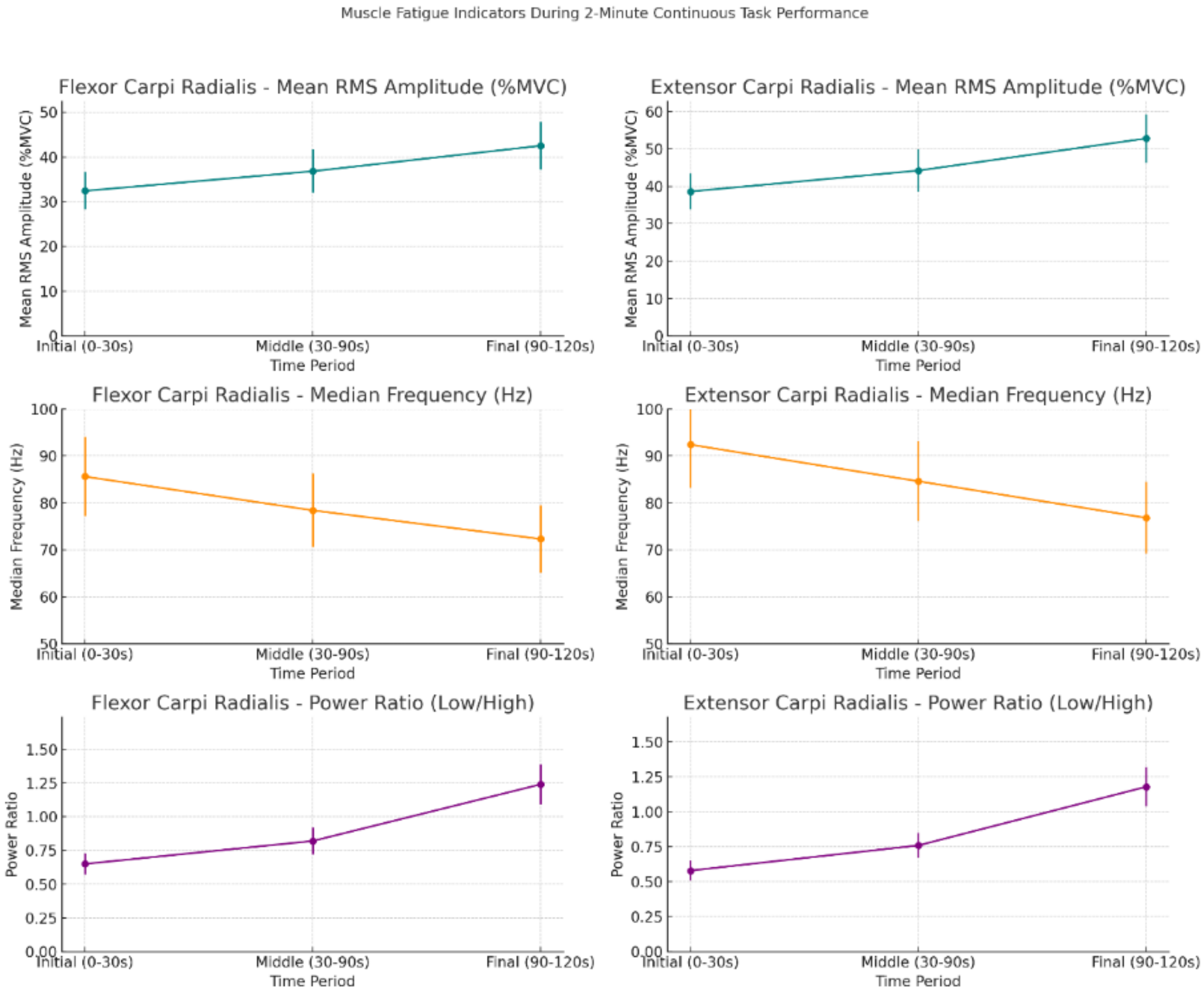

Figure 5. Muscle fatigue indicators during 2-min continuous task performance.

The task-specific fatigue characteristics presented in **Table 15** demonstrated varying rates of fatigue development across different brushstroke types. Stippling showed the highest fatigue development rate (22.8 ± 2.8 %/min) and required the longest recovery time (52.6 ± 6.5 s) while exhibiting the shortest endurance time (82.4 ± 10.4 s). In contrast, fine detail work demonstrated the lowest fatigue development rate (12.6 ± 1.6 %/min) and shortest recovery time (32.4 ± 4.2 s), with the longest endurance time (112.8 ± 14.2 s), suggesting that lower-intensity, precise movements could be sustained for more extended periods despite the high attention demands.

Table 15. Task-specific fatigue development rates and recovery indicators.

Task Type	Fatigue Development Rate (%/min)	Recovery Time (s)	Endurance Time (s)
Broad Strokes			
Mean ± SD	18.4 ± 2.3	45.6 ± 5.8	94.5 ± 11.8
Range	14.2–22.6	35.2–56.4	74.8–114.2
Fine Detail			
Mean ± SD	12.6 ± 1.6	32.4 ± 4.2	112.8 ± 14.2
Range	9.8–15.4	24.8–40.2	88.5–136.4
Stippling			
Mean ± SD	22.8 ± 2.8	52.6 ± 6.5	82.4 ± 10.4
Range	17.6–28.2	40.8–64.5	64.2–100.6
Circular			
Mean ± SD	15.6 ± 1.9	38.5 ± 4.8	104.6 ± 13.2
Range	12.2–19.2	29.8–47.2	82.4–126.8

6.6. Kinematic and kinetic efficiency analysis

Analysis of movement efficiency metrics in **Table 16** and **Figure 6** revealed significant differences across brushstroke types ($p < 0.001$). Broad strokes showed the highest energy cost (4.82 ± 0.62 J/m) and path ratio (1.24 ± 0.15), indicating lower movement economy compared to other techniques. Fine detail and stippling demonstrated superior movement precision, with spatial errors of 0.84 ± 0.10 mm and 0.62 ± 0.08 mm, respectively, significantly lower than broad strokes (3.86 ± 0.48 mm) and circular movements (2.45 ± 0.32 mm). The task-specific performance parameters presented in **Table 17** and **Figure 7** showed distinct movement control and efficiency patterns. Fine detail work exhibited the highest feedback gain (0.92 ± 0.11) and a high correction rate (8.6 ± 1.1 Hz), reflecting the increased control demands of precise movements. Stippling demonstrated the lowest efficiency ratio (8.3% ± 1.0%) but the highest correction rate (12.4 ± 1.5 Hz), suggesting a trade-off between metabolic efficiency and movement control. Broad strokes achieved the highest efficiency ratio (19.9% ± 2.5%) despite their higher absolute energy cost, indicating better energy utilization during large-scale movements.

Table 16. Movement efficiency metrics across brushstroke types (N = 21).

Efficiency Parameter	Broad Strokes	Fine Detail	Stippling	Circular	F-value	p-value
Movement Economy						
Energy Cost (J/m)	4.82 ± 0.62	2.34 ± 0.28	1.86 ± 0.24	3.45 ± 0.42	38.64	< 0.001
Path Ratio	1.24 ± 0.15	1.08 ± 0.12	1.04 ± 0.11	1.18 ± 0.14	25.32	< 0.001
Movement Precision						
Spatial Error (mm)	3.86 ± 0.48	0.84 ± 0.10	0.62 ± .08	2.45 ± 0.32	42.18	< 0.001
Temporal Variability (%)	12.4 ± 1.5	8.6 ± 1.1	6.8 ± 0.9	10.2 ± 1.3	34.75	< 0.001

Table 17. Task-specific performance and control parameters.

Control Parameter	Broad Strokes	Fine Detail	Stippling	Circular
Movement Time (s)				
Mean ± SD	1.24 ± 0.15	0.48 ± 0.06	0.06 ± 0.01	0.82 ± 0.10
Optimal	1.08 ± 0.13	0.42 ± 0.05	0.05 ± 0.01	0.74 ± 0.09
Muscle Efficiency				
Work Output (J)	0.86 ± 0.11	0.24 ± 0.03	0.12 ± 0.02	0.58 ± 0.07
Metabolic Cost (J)	4.32 ± 0.54	1.85 ± 0.23	1.45 ± 0.18	3.24 ± 0.41
Efficiency Ratio (%)	19.9 ± 2.5	13.0 ± 1.6	8.3 ± 1.0	17.9 ± 2.2
Control Strategy				
Feedback Gain	0.68 ± 0.08	0.92 ± 0.11	0.84 ± 0.10	0.76 ± 0.09
Correction Rate (Hz)	4.2 ± 0.5	8.6 ± 1.1	12.4 ± 1.5	6.8 ± 0.8

* Note: Efficiency Ratio = (Work Output/Metabolic Cost) × 100; Feedback Gain ranges from 0 (Low Control) to 1 (High Control)

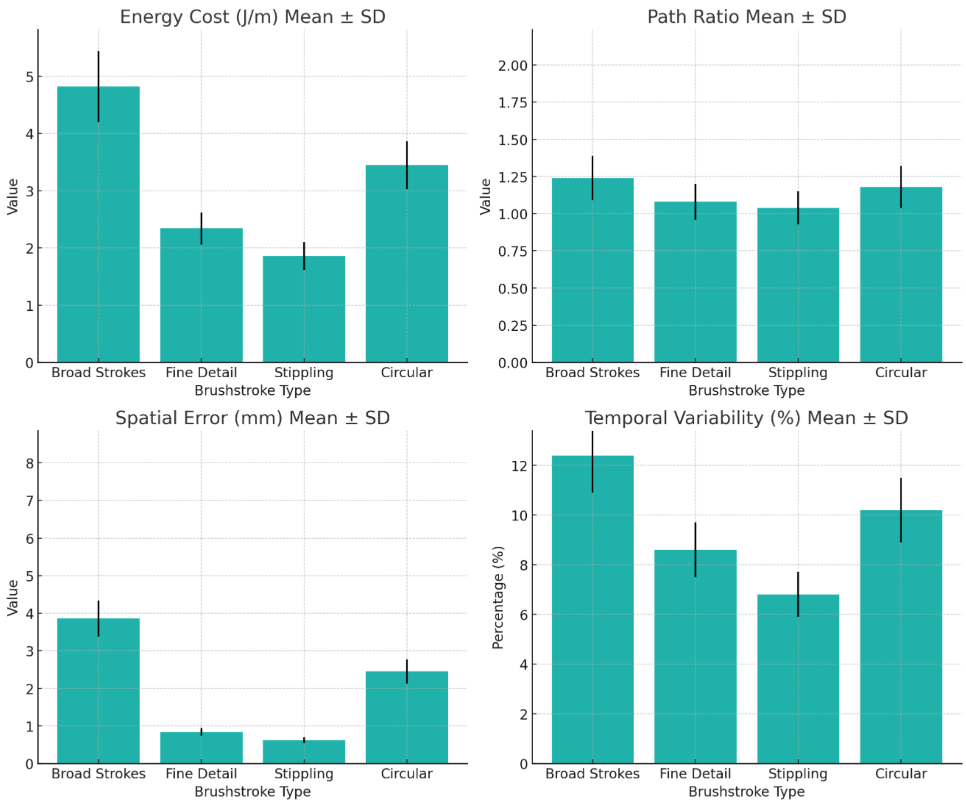

Figure 6. Movement efficiency metrics across brushstroke types.

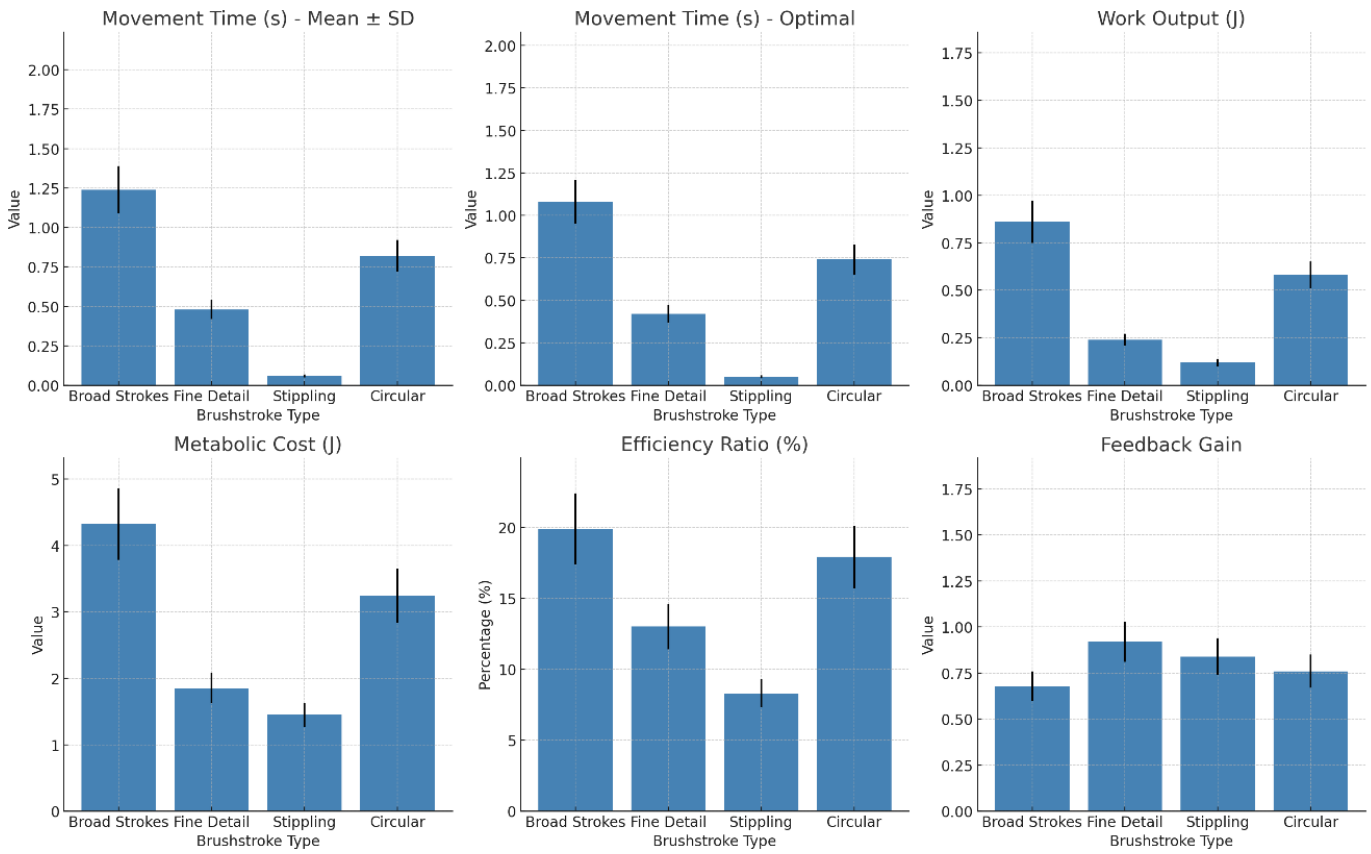

Figure 7. Task-specific performance and control parameters.

The biomechanical cost of moving through the paint space refers to the cost of joint motion, or the least amount of effort needed to control the movement. Feedback gain relates to the sensorimotor loop needed to make corrections based on what is sensed when the hand is in movement to obtain the expected results regardless of the movement. The high correction rates mean that the proprioceptive feedback is good, but the high correction rate may be inefficient if it has to be corrected too often. Sophisticated biomechanical models estimate positions and velocities, even reaction time and precision rate, and measure performance and learning adaptations. Underlining such stable hand trajectory and smooth acceleration patterns increases kinematic efficiency, making it easy to master artistic works.

The biomechanical effects of painting materials differ significantly. Oil painting is more of a constant muscular work because paint application entails thicker brushes and dries slowly than acrylics; it entails constant grip force and stability, resulting in wrist and shoulder straining. Because of its loose strokes and free-flowing movements, Watercolor does not overly apply and maintain tension but requires fine muscle control. Acrylics have some characteristics of both, requiring somewhat above-average endurance and control. Fresco painting is predominantly an overhead job, increasing shoulder and neck strain chances. These effects are magnified with tools, including brush size and canvas orientation. For instance, horizontal canvases and larger brushes contribute to more shoulder movement, while small brushes generally require wrist movement.

7. Conclusion and future work

This study examined the biomechanical aspects of brushstroke dynamics in painting, focusing on the physical requirements of different brushstroke techniques. Through integrating motion capture, force sensors, and electromyography, we captured detailed data on joint angles, muscle activation, and force application across broad, fine-detail, stippling, and circular strokes. The findings demonstrate that each brushstroke type imposes distinct biomechanical demands influenced by the range of motion, muscle engagement, and force consistency. Broad strokes required substantial shoulder and elbow involvement, allowing for expansive, fluid movements but also placing increased demand on larger muscle groups. On the other hand, fine detail strokes relied heavily on precise wrist and finger control, which required high levels of stability and dexterity. The repetitive stippling strokes increased force levels and muscle activation, suggesting an increased fatigue risk over extended sessions. Circular strokes combine linear and rotational movements, activating the forearm and wrist muscles and showcasing the complex motor coordination needed for smooth, continuous motions. These insights highlight the importance of understanding the biomechanics of painting to improve technique, enhance endurance, and minimize strain. For art practitioners, incorporating knowledge of joint angles, force distribution, and muscle activation patterns can inform more sustainable painting practices. In addition, this research provides a foundation for developing ergonomic guidelines and targeted training programs, which may benefit artists and art educators aiming to optimize technique while preventing injury. In conclusion, this study establishes a baseline for understanding the physical demands of painting from a biomechanical perspective, bridging the gap between art and science.

Future research could extend this analysis to other forms of visual art, consider different artistic tools and mediums, and explore long-term muscle and joint function adaptations in professional artists. This work contributes to a holistic understanding of the biomechanics behind creative practice by exploring the intricate relationship between physical motion and artistic expression.

Ethical approval: Not applicable.

Conflict of interest: The author declares no conflict of interest.

References

1. An Z, and Nie D. Impact Of Chinese Cultural Elements on Spiritual Expression in Oil Painting Imagery Landscape: An Exploratory Study in Arts Education. Arts Educa. 2023; 37.
2. da Mota Gomes[1], M. Exploring the Art and Experiences of Painters with Epilepsy. Revista Brasileira De. 2023; 59(4 Suppl 1), 63103.
3. Cereda F. Movement as the core of physical engagement and understanding. 2024.
4. DeLauder RM. Movement Through the Storm: Integrating Dance and Biomechanical Principles in Dance/Movement Therapy Services for People with Multiple Sclerosis (Doctoral dissertation, Drexel University). 2021.
5. Breuer S, Braun M, Tigard D, Buyx A, and Müller R. How engineers' imaginaries of healthcare shape design and user engagement: A case study of a robotics initiative for geriatric healthcare AI applications. ACM Transactions on Computer-Human Interaction. 2023; 30(2), 1–33.
6. Iandoli L, and Zollo G. Elegant Design: A Designer's Guide to Harnessing Aesthetics. Bloomsbury Publishing. 2022.

7. Spee BT, Mikuni J, Leder H, Scharnowski F, Pelowski M, and Steyrl D. Machine learning revealed symbolism, emotionality, and imaginativeness as primary predictors of creativity evaluations of Western art paintings. Scientific Reports. 2023; 13(1), 12966.
8. Pellegrini B, Hettinga FJ, Mourot LD, Vernillo G, and Schena F. State of the art and perspectives of sports science in the run-up to the Milano Cortina 2026 Olympic Winter Games. Sport Sciences for Health. 2023; 19(4), 1039–1042.
9. Berkmans F, Robache F, Mironova A, Nys L, Wieczorowski M, and Bigerelle M. Brushes and brains: Does handedness influence surface topography of art painting?. Measurement. 2024; 230, 114521.
10. Borghini A, and Ferretti G. Dip It before You Eat It! On Recipes and the Architecture of a Dish. A Philosophy of Recipes: Making, Experiencing, and Valuing. 2022; 57.
11. Rabah A, Le Boterff Q, Carment L, Bendjemaa N, Térémetz M, Dupin L, ... and Lindberg PG. A novel tablet-based application for assessment of manual dexterity and its components: a reliability and validity study in healthy subjects. Journal of Neuro Engineering and Rehabilitation. 2022; 19(1), 35.
12. Garofalo S, Morano C, Perrelli M, Pagnotta L, Carbone G, Mundo D, and Bruno L. A critical review of transitioning from conventional actuators to artificial muscles in upper-limb rehabilitation devices. Journal of Intelligent Material Systems and Structures. 2024; 35(16), 1263–1290.
13. Sharma B, Phan PT, Davies J, Hoang TT, Nguyen CC, Ji A, ... and Do TN. Soft Upper-Limb Wearable Robotic Devices: Technology and Applications. Advanced Intelligent Systems. 2024; 2400266.
14. Krakauer JW, and Carmichael ST. Broken movement: the neurobiology of motor recovery after stroke. MIT Press. 2022.
15. Rosales E, Araújo C, Rodriguez J, Vining N, Yoon D, and Sheffer A. AdaptiBrush: adaptive general and predictable VR ribbon brush. ACM Trans. Graph. 2021; 40(6), 247–1.
16. Hedlund Nelson M. Art, movement and the body: An art-based research exploration of slow, gentle, and repetitive painting movements. 2020.
17. Sonning A. Creative Concert Production and Entrepreneurship: Concert Dramaturgy and Project Development for the Performing Arts. Taylor & Francis. 2024.
18. Pinos K. The Synesthetic Language of Picasso: Exploring Emotions and Sensations in His Art. American Journal of Multidisciplinary Research and Innovation. 2024; 3(4), 118–129.
19. Cho Y. Painterly Hybridisation: Re-presenting Oriental Painting as an Intercultural Hybrid (Doctoral dissertation, The Glasgow School of Art). 2023.
20. Liu Y, Hu W, Kasal A, and Erdil YZ. The State of the Art of Biomechanics Applied in Ergonomic Furniture Design. Applied Sciences. 2023; 13(22), 12120.
21. Yough M. Advancing Medical Technology for Motor Impairment Rehabilitation: Tools, Protocols, and Devices (Doctoral dissertation, West Virginia University). 2023.
22. Mishra N, Habal BGM, Garcia PS, and Garcia MB. Harnessing an AI-Driven Analytics Model to Optimize Training and Treatment in Physical Education for Sports Injury Prevention. In Proceedings of the 2024 8th International Conference on Education and Multimedia Technology (pp. 309–315). 2024.
23. Daley D, Payne LP, Galper J, Cheung A, Deal L, Despres M, ... and Escorpizo R. Clinical Guidance to Optimize Work Participation After Injury or Illness: The Role of Physical Therapists: Clinical Practice Guidelines Linked to the International Classification of Functioning, Disability and Health From the Academy of Orthopaedic Physical Therapy of the American Physical Therapy Association. Journal of Orthopaedic & Sports Physical Therapy. 2021; 51(8), CPG1-CPG102.
24. Nallathambi I, Savaram P, Sengan S, et al., Impact of Fireworks Industry Safety Measures and Prevention Management System on Human Error Mitigation Using a Machine Learning Approach, Sensors, 2023, 23 (9), 4365; DOI:10.3390/s23094365.
25. Krishnamoorthy P, Satheesh N, Sudha D, et al. Effective Scheduling of Multi-Load Automated Guided Vehicle in Spinning Mill: A Case Study, IEEE Access, 2023, 11, 9389–9402. DOI:10.1109/ACCESS.2023.3236843.
26. Ran Q, Sengan S, Juneja S. English language teaching based on big data analytics in augmentative and alternative communication system, Springer-International Journal of Speech Technology, 2022, 25, 409–420. DOI:10.1007/s10772-022-09960-1.
27. Ngangbam PS, Suman S, Ramachandran TP, et al. Investigation on characteristics of Monte Carlo model of single electron transistor using Orthodox Theory, Elsevier, Sustainable Energy Technologies and Assessments, Vol. 48, 2021, 101601, DOI:10.1016/j.seta.2021.101601.

28. Huang H, Wang X, Sengan S, Chandu T. Emotional intelligence for board capital on technological innovation performance of high-tech enterprises, Elsevier, Aggression and Violent Behavior, 2021, 101633, DOI:10.1016/j.avb.2021.101633.
29. Sengan S, Kumar K, Subramaniyaswamy V, Ravi L. Cost-effective and efficient 3D human model creation and re-identification application for human digital twins, Multimedia Tools and Applications, 2021, 81(19), 26839–26856. DOI:10.1007/s11042-021-10842-y.
30. Narayanan P, Sengan S, Marimuthu BP, Paulra RK. Novel Collision Detection and Avoidance System for Mid-vehicle Using Offset-Based Curvilinear Motion. Wireless Personal Communication, 2021, 119(3), 2323–2344. DOI:10.1007/s11277-021-08333-2.
31. Alphonse, B., Rajagopal, V., Sengan, S. et al. Modeling and multi-class classification of vibroarthographic signals via time domain curvilinear divergence random forest, J Ambient Intell Human Comput, 2021, DOI:10.1007/s12652-020-02869-0.
32. Neffati OS, Setiawan R, Jayanthi P, et al. An educational tool for enhanced mobile e-Learning for technical higher education using mobile devices for augmented reality, Microprocessors and Microsystems, 83, 2021, 104030, DOI: 10.1016/j.micpro.2021.104030.
33. Ayasrah FT, Alsharafa FS, S S, et al. Strategizing Low-Carbon Urban Planning through Environmental Impact Assessment by Artificial Intelligence-Driven Carbon Foot Print Forecasting, Journal of Machine and Computing, 2024, 4(4), 1140–1151 doi: 10.53759/7669/jmc202404105.
34. Nowfal SH, Sadu VB, Sengan S, et al., Genetic Algorithms for Optimized Selection of Biodegradable Polymers in Sustainable Manufacturing Processes, Journal of Machine and Computing, 2024, 4(3), 563–574, https://doi.org/10.53759/7669/jmc202404054.
35. Ghanimi HMA, Sengan S, Sadu VB, et al. An open-source MP + CNN + BiLSTM model-based hybrid model for recognizing sign language on smartphones. Int J Syst Assur Eng Manag. 2024, 15, 3794–3806. https://doi.org/10.1007/s13198-024-02376-x
36. Bhavana Raj K, Webber JL, Marimuthu D, et al. Equipment Planning for an Automated Production Line Using a Cloud System, Innovations in Computer Science and Engineering. ICICSE 2022. Lecture Notes in Networks and Systems, 565, 707–717, Springer, Singapore. DOI:10.1007/978-981-19-7455-7_57.